2011

Prediction of Brain Tumor Progression Using Multiple Histogram Matched MRI Scans

Debrup Banerjee
Old Dominion University

Loc Tran
Old Dominion University

Jiang Li
Old Dominion University, jli@odu.edu

Yuzhong Shen
Old Dominion University, yshen@odu.edu

Frederic McKenzie
Old Dominion University, rdmckenz@odu.edu

See next page for additional authors

Original Publication Citation

Banerjee, D., Tran, L., Li, J., Shen, Y., McKenzie, F., & Wang, J. (2011).Prediction of brain tumor progression using multiple histogram matched MRI scans. In R.M. Summers & B.V. Ginneken (Eds.), *Medical Imaging 2011: Computer-Aided Diagnosis, Proceedings of SPIE Vol. 7963* (79632U). SPIE of Bellingham, WA. https://doi.org/10.1117/12.878208

Prediction of Brain Tumor Progression using Multiple Histogram Matched MRI Scans

Debrup Banerjee[a], Loc Tran[a], Jiang Li*[a], Yuzhong Shen[a], Frederic McKenzie[a] and Jihong Wang[b]
[a]Department of ECE, Old Dominion University, Norfolk, VA 23529, USA
[b]Diagnostic Imaging, University of Texas MD Anderson Cancer Center, Houston, Texas 77030

ABSTRACT

In a recent study [1], we investigated the feasibility of predicting brain tumor progression based on multiple MRI series and we tested our methods on four patients' MRI images scanned at three consecutive visits A, B and C. Experimental results showed that it is feasible to predict tumor progression from visit A to visit C using a model trained by the information from visit A to visit B. However, the trained model failed when we tried to predict tumor progression from visit B to visit C, though it is clinically more important. Upon a closer look at the MRI scans revealed that histograms of MRI scans such as T1, T2, FLAIR etc taken at different times have slight shifts or different shapes. This is because those MRI scans are qualitative instead of quantitative so MRI scans taken at different times or by different scanners might have slightly different scales or have different homogeneities in the scanning region. In this paper, we proposed a method to overcome this difficulty. The overall goal of this study is to assess brain tumor progression by exploring four patients' complete MRI records scanned during their visits in the past two years. There are ten MRI series in each visit, including FLAIR, T1-weighted, post-contrast T1-weighted, T2-weighted and five DTI derived MRI volumes: ADC, FA, Max, Min and Middle Eigen Values. After registering all series to the corresponding DTI scan at the first visit, we applied a histogram matching algorithm to non-DTI MRI scans to match their histograms to those of the corresponding MRI scans at the first visit. DTI derived series are quantitative and do not require the histogram matching procedure. A machine learning algorithm was then trained using the data containing information from visit A to visit B, and the trained model was used to predict tumor progression from visit B to visit C. An average of 74% pixel-wise accuracy was achieved for tumor progression prediction from visit B to visit C.

Keywords: Histogram Matching, Predicting Brain Tumor Progression, DTI

1. INRODUCTION

The usefulness of prediction of brain tumor progression is in its early detection, prevention and clinical therapy. It is known that different modalities of magnetic resonance imaging techniques can focus on various structural features in the brain. A relatively comprehensive profile of brain structures can thus be represented from the feature combination of several imaging modalities. Advanced MRI techniques are being evaluated for their ability to improve delineation of glioma boundaries and predict regions of future growth that are not apparent in conventional T2-weighted and post contrast T1-weighted MRI. Wright et al. have compared the spatial distribution of anomalous regions of isotropic and anisotropic components of water diffusion in gliomas and their surrounding edema, using diffusion tensor imaging (DTI) [2]. The diagnosis of brain tumors by magnetic resonance imaging (MRI) is usually based on basic unenhanced T1- and T2-weighted images or post-contrast T1-weighted images. Conventional MRI techniques are not sufficient for the grading and specification of brain tumors because of its lack of specificity.

Additional imaging techniques have been utilized to overcome this problem. Nowadays, tumors can be further characterized by using, e.g., dynamic contrast-enhanced imaging, delayed imaging, magnetization transfer techniques, contrast-enhanced fast FLAIR MRI, perfusion-weighted MRI and MR spectroscopy [3]. In diffusion-weighted imaging (DWI), the image contrast is determined by the random translational (Brownian) motion of water molecules. Diffusion imaging also provides indirect structural information that is not available from basic MRI sequences, which may reveal further pathological conditions [3]. A change detection algorithm has been proposed by Patriarche and Erickson [4] to quantitatively compare, detect and characterize changes in serial magnetic resonance imaging studies of brain tumor patients. By employing the Mahalanobis distance-based metric, the voxels of one of the two tissues, normally appearing white matter (NAWM) and non-enhancing T2 abnormality (NETTA), were classified.

* Email: JLi@odu.edu.

Medical Imaging 2011: Computer-Aided Diagnosis, edited by Ronald M. Summers, Bram van Ginneken,
Proc. of SPIE Vol. 7963, 79632U · © 2011 SPIE · CCC code: 0277-786X/11/$18 · doi: 10.1117/12.878208

In this particular study, four brain tumor patients underwent multiple visits over a time span of two years. The patients underwent multiple magnetic resonance imaging studies at each visit that included FLAIR, post-contrast *T*1-weighted , *T*1-weighted, *T*2-weighted, and DTI. For each DTI scan, five scalar maps were derived (ADC, FA, Max, Min and Middle Eigen Value) yielding a total of 10 image series for each patient. All series were co-registered to the corresponding DTI series at the first visit. After registering all series to the corresponding DTI scan at the first visit, we applied a histogram matching algorithm to non-DTI MRI scans to match their histograms to those of the corresponding MRI scans at the first visit. In this study, we focused on the trend of brain tumor progression during three consecutive visits, i.e., visit A, visit B and visit C. The intensity-based features of each pixel inside annotated regions of interest at each visit were extracted across all 10 co-registered imaging series and concatenated to a 10-dimensional vector. Each of these feature vectors can fall into one of the three categories: normal, tumor, and normal but progressed to tumor at the next visit. A multilayer perceptron (MLP) with an adaptive learning factor [5], was trained using data containing information from visit A to visit B, and the trained model was used to predict tumor progression from visit B to visit C. An average of 72% pixel-wise accuracy was achieved for tumor progression prediction from visit B to visit C using the histogram matched MRI series. The paper is organized as follows. The proposed method of brain tumor progression assessment is detailed in Section 2. Experiments are described in Section 3. Prediction results are given in Section 4. Discussions are presented in Section 5 and we conclude this paper in Section 6.

2. METHODOLOGY

2.1 Data Preparation

Four brain tumor patients were selected retrospectively from a patient cohort who underwent multiple visits over the time span of two years. At each visit, patients underwent multiple MR imaging studies including FLAIR, T1-weighted, post-contrast T1-weighted, T2-weighted, and DTI. For each DTI scan, five calculated scalar maps were derived (ADC, FA, Max, Min and Middle Eigen Values) yielding 10 image series for each patient at each visit. The interval between two visits was one or two months. All series were co-registered to the corresponding DTI series at the first visit. Annotated normal and tumor regions were defined on either FLAIR or post-contrast T1-weitghted MR and then overlaid to other registered MRI slices at the same visit. The patient selection criterion includes that they have visible brain tumor regions on either FLAIR or post-const T1 slices taken at three visits and the tumor regions were expanding along with time.

2.2 Registration

For a particular visit, all series were first rigidly registered to the T1 scan of that visit to remove any intra-visit motion. This process was repeated for all visits. In order to remove inter-visit motion, only the T1 scan from each subsequent visit was rigidly registered to the T1 scan from the first visit. As a post processing step, for all registrations, the brain was automatically extracted from the T1 reference scan (using the Brain Extraction Tool (BET)) so that only the brain was aligned during the registration process. Due to the multimodal nature of the registration task, Normalized Mutual Information was the similarity measure chosen. All registrations were performed using the freeware vtkCISG registration toolkit, developed at King's College London [6]. By combining the registration transforms from the intra- and inter-subject registration results, we have the ability to align every series from every visit to a visit and series of our choice. For this work, we chose to align every series from every visit to the DTI scan at the first visit. We should emphasize that it is not necessary to separately register DTI derived series (FA, ADC, Max, Min and Middle Eigen value) because they can be aligned by utilizing transforms resulting from the original DTI registrations.

2.3 Histogram Matching

The registered non-DTI MRI scans were converted to histogram matched scans to the corresponding images at the first visit using a standard histogram matching algorithm as follows. Given two images, the reference and the target image to be adjusted, we first computed their histograms and the cumulative functions as $F1()$ and $F2()$, for the reference and target images, respectively. Then for each gray level, $G2$, in the target image, we found a gray level, $G1$, in the reference image such that $F1(G1) = F2(G2)$, and $G2$ was replaced by the gray level $G1$. As a result, the histogram of the modified target image will be, ideally, the same as the histogram of the reference image.

2.4 Feature Extraction

For each patient, we used $I(t;m;n)$ to represent the nth histogram matched image slice in the mth imaging series at his/her tth visit. After the registration, $I(t';m';n)$ was aligned with $I(1;DTI;n)$ for all $t' \epsilon V$ and $m' \epsilon M$ where V is this patient's

total number of visits, and M is the total number of imaging series at the tth visit. At a particular visit t, when we examined a region of interest (ROI) in $I(t;m;n)$ we could find the corresponding region in $I(t';m';n)$ for all m. A feature vector was used to represent the intensity-based features of pixel p inside the ROI as $x_p = \{x_{p1}, x_{p2}, \ldots, x_{pM}\}_{p=1}^{N_v}$ where $\boldsymbol{x}_{pm}$ *(m=1,2,3…,M)* is the intensity value of pixel p in $I(t;m;n)$. For the N_v collected feature vectors $\{x_p, i_p\}_{p=1}^{N_v}$ where x_p $\in$ $R^{\mathbf{M}}$, i_p $\in$ I, each feature vector fell into one of the three classes: normal (i_p = 1), tumor (i_p = 2), and normal but progressed to tumor at a later time (i_p = 3) [1].

2.5 Training and Testing

Neural network classifiers trained using the mean squared error (MSE) objective function have been shown to approximate the optimal Bayesian classifier. Given the collected feature vectors, we convert $\mathbf{i}_p$ to a real vector $\mathbf{t}_p \in \boldsymbol{R}^{Nc}$ as $\boldsymbol{t}_p(i_c) = 1$ and $\boldsymbol{t}_p(i_d) = -1$, where i_c denotes the correct class number for the current $\mathbf{x}_p$, i_d denotes any incorrect class number for x_p, and $\boldsymbol{N}_c$ is the number of classes ($\boldsymbol{N}_c = 3$ in this study). The classifier was designed by mapping $\mathbf{x}$ to $\mathbf{t}$. We designed a multi-layer perceptron (MLP) consisting of an input layer, a hidden layer, and an output layer for the classification by minimizing the standard MSE cost function. To solve the hidden weights we utilized the back propagation (BP) algorithm combined with the output reset (OR) method [5].

3. EXPERIMENTS

Three visits for each of the four patients were selected in this study, namely Visit A, B and C. An MLP classifier [5] was then trained using the collected feature vectors containing information from visit A to visit B, and the trained model was then applied to predict tumor progression from visit B to visit C. The MLP classifier had 10 inputs, six hidden unites and three outputs. The MLP was trained for 200 iterations. All non-DTI MRI slices' histograms were matched.

4. RESULTS

Figure 1 shows one example of histogram matching result. The registered FLAIR images in Figures 1(a) and 1(b) were taken at different visits and so have different histograms as shown in Figure 2. The task here is to modify image in Figure 1(b) such that its histogram will be matched to the histogram of the reference image shown in Figure 1(a). Figure 1(c) shows the histogram matched image and its corresponding histogram is shown in Figure 2. The same technique was applied to other non-DTI image series and more examples are shown in Figures 3 and 4.

Figure 5 shows one example slice of the prediction results. Figure 5(a) illustrates the post contrast T1-wighted MRI image slice at visit A. Figure 5(b) illustrates the image slice at visit B. Figure 5(c) illustrates the images slice at visit C. Normal (green), tumor (red) and progression (yellow) regions were manually annotated on FLAIR slices but overlaid on the post contrast T1-wighted image slices as shown in Figure 5(a)-(c). We utilized information from visit A to visit B to train a model and predicted the tumor progression from visit B to visit C using the trained model. Figure 5(d) shows the prediction result. Figures 6-9 show more prediction results.

Figure 10 illustrates the prediction results where the tumor contours were defined on the post-contrast T1-weighted image slices, another non-DTI based modality. Figures 10(a) and (e) illustrate the post contrast T1-weighted image slices at visit A. Figures 10(b) and (f) illustrate the post contrast T1-weighted image slices at visit B. Figures 10(c) and (g) illustrate the post contrast T1-weighted image slices at visit C. Normal (green), tumor (red) and progression (yellow) regions were manually annotated as shown in Figures 10(a)-(c) and 10(e)-(g). Figures 10(d) and (h) show the corresponding prediction results. Note that there are multiple slices for each patient on which tumors are visible and here only one slice is shown for some of the patients.

Figure 11 shows one failed case for the prediction where the tumor contours were defied on the post-contract T1-weighted MR slices. At visit C, most of the normal regions were predicted as either tumor or progressed regions. Note that there are many highlighted regions at visit B (Figure 11b and 11f) and those in the annotated normal region are different from the corresponding region at visit A (Figure 11a and 11e). We suspect this is the reason the normal regions were classified as either tumor or progressed regions at visit C (Figure 11d and 11h).

An average of 77% pixel-wise accuracy was achieved for the four patients if tumor contours were defined on FLAIR slices while an average of 70% pixel-wise accuracy was obtained if tumor regions were defined on post-contract T1-weighted slices. Overall, the accuracy for the tumor progression prediction was 74%.

5. DISCUSSION

Intensity-based feature vectors of pixels inside annotated brain tumors and surrounding regions were utilized in this study. The prediction results were generally consistent with the manually marked contours showing the primary progressing directions of the tumors. The promising results demonstrate the feasibility of predicting the progression of brain tumor utilizing histogram matched MRI scans. We expect better prediction results if more information from the MRI scans were included.

In this study, the regions of tumor, progressing and normal tissues were manually annotated on FLAIR and post-contrast T1-weighed images, respectively. Brain tumors on FLAIR images are relatively the most visually distinguishable. However, even on FLAIR images, the boundaries of brain tumors are still often not clear, which is a characteristic of malignant brain tumors. Therefore, normal tissue close to the tumor boundary might be mislabeled as tumor, which will lead to degradation of the prediction accuracy.

6. CONCLUSION

We have implemented a standard histogram-matching algorithm to match non-DTI MRI scans taken at different visits and by different scanners. Preliminary results show that it is feasible to perform one-step forward prediction for brain tumor progression based on multiple histogram matched MRI series. Our future work includes recruiting more patients for the study, characterizing tumor boundaries using unsupervised learning techniques and performing sensitivity analysis for deferent MRI scans.

REFERENCES

[1]. Shen, Y., Li, J., Chandler, A., Shen, Y., McKenzie, F.D. and Wang, J., "Prediction of Brain Tumor Progression using a Machine Learning Technique", in Proceedings of SPIE Medical Imaging, 2010.

[2]. Wright, A.J., Fellows, G., Byrnes, TJ., Opstad, K.S., McIntyre, D.J., Griffiths, J.R., Bell, B.A., Clark, C.A., Barrick, T.R. and Howe, F.A., "Pattern Recognition of MRSI Data Shows Regions of Glioma Growth That Agree With DTI Markers of Brain Tumor Infiltration", Magnetic Resonance in Medicine, vol. 62, no. 6, pp. 1646-51, 2009.

[3]. Bode, M.K., Ruohonen, J., Nieminen, M.T. and Pyhtinen, J., "Potential of Diffusion Imaging in Brain Tumors: A Review", Acta Radiologica, vol. 47, no. 6, pp. 585–594, 2006.

[4]. Patriarche, J.W. and Erickson, B. J., "Automated Change Detection and Characterization in Serial MR Studies of Brain-Tumor Patients", Journal of Digital Imaging, vol. 20, no. 3, pp. 203-222, 2006.

[5]. Li, J., Manry, M. T., Liu, L. M., Yu, C., and Jiang, W., "Iterative improvement of neural classifiers," in Proceedings of the Seventeenth International Conference of the Florida AI Research Society, pp. 700-705, May, 2004.

[6]. Hartkens, T., Ruechert, D., Schnabel, J. A., Hawkes, D. J., and Hill, D. L. G., "VTK CISG Registration Toolkit: An open source software package for affine and non-rigid registration of single- and multimodal 3D images," in Workshop Bildverarbeitung fÄur die Medizin, pp. 409-412, 2002.

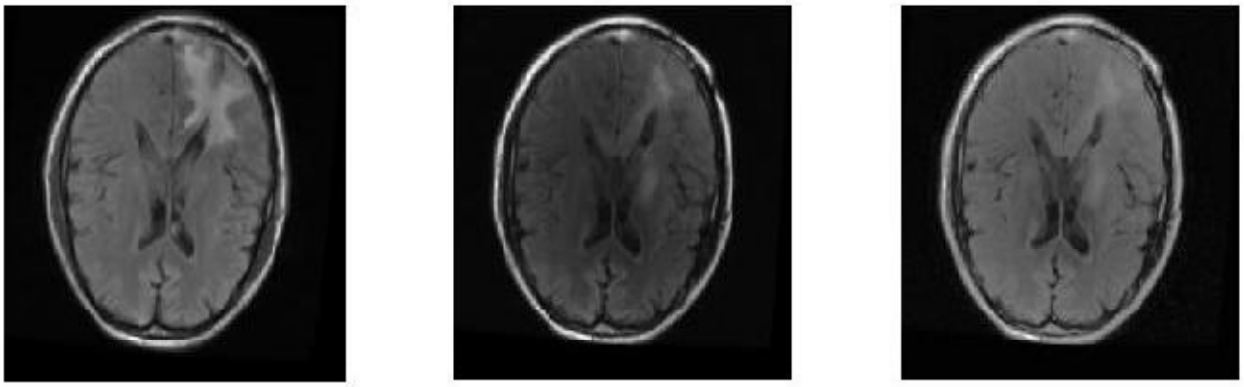

(a) (b) (c)

Figure 1. Histogram matching result for one sample FLAIR image. a) reference image, b) target image and c) histogram matched target image.

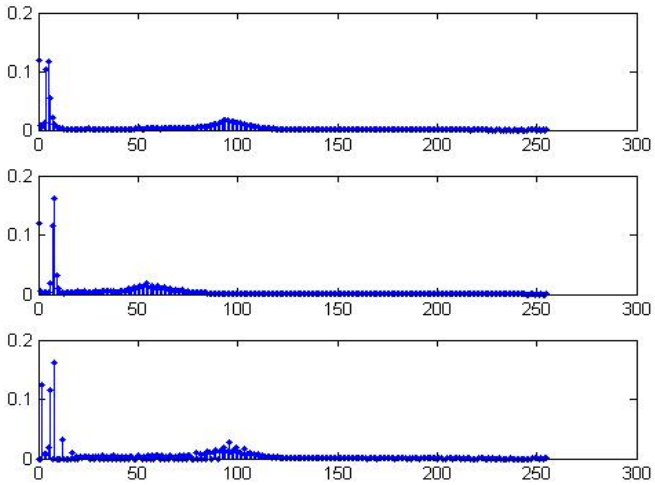

Figure 2. Histograms for the images shown in Figure 1. top: histogram of the image shown in Figure 1 (a), middle: histogram of the image shown in Figure 1 (b), bottom: histogram of the matched image shown in Figure 1 (c).

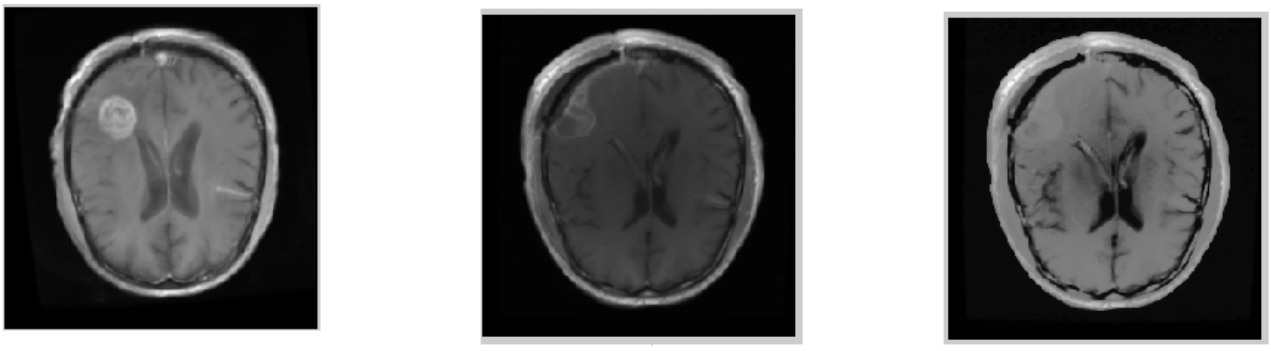

(a) (b) (c)

Figure 3. Histogram matching result for a sample post contrast T1-weighted image. (a) reference image, (b) target image and (c) histogram matched target image.

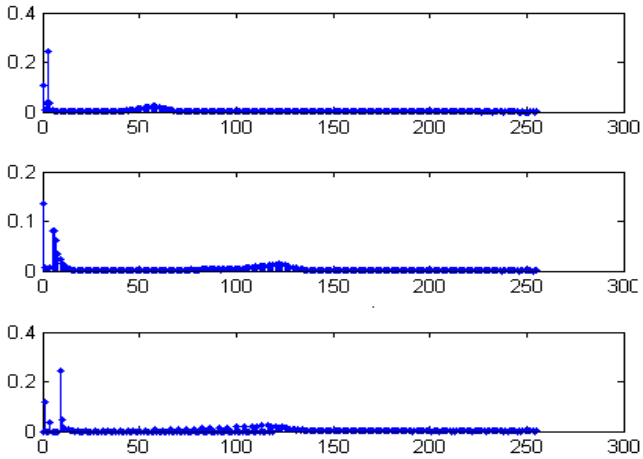

Figure 4. Histograms for the images shown in Figure 3. top: histogram of the image shown in Figure 3 (a), middle: histogram of the image shown in Figure 3 (b), bottom: histogram of the matched image shown in Figure 3 (c).

(a) (b) (c) (d)

Figure 5. Prediction of brain tumor progression using histogram matched MRI images. (a)-(c), Manually annotated contours on FLAIR, normal (green), tumor (red) and progression (yellow) at visit A, B and C, respectively, overlaid on the post contrast T1-wighted MRI slice (d) Predicted results at visit C using data at visit B (in Figure 5b) as inputs to the trained model.

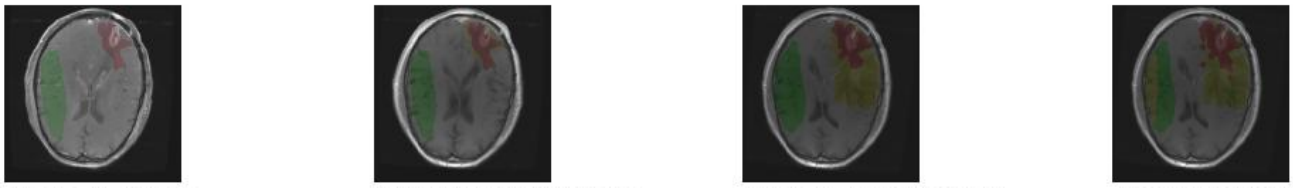

(a) (b) (c) (d)

Figure 6. Prediction result on one sample slice for another patient. Images are arranged the same way as that in Figure 5.

.

(a) (b) (c) (d)

Figure 7. Prediction result on one sample slice for another patient. Images are arranged the same way as that in Figure 5.

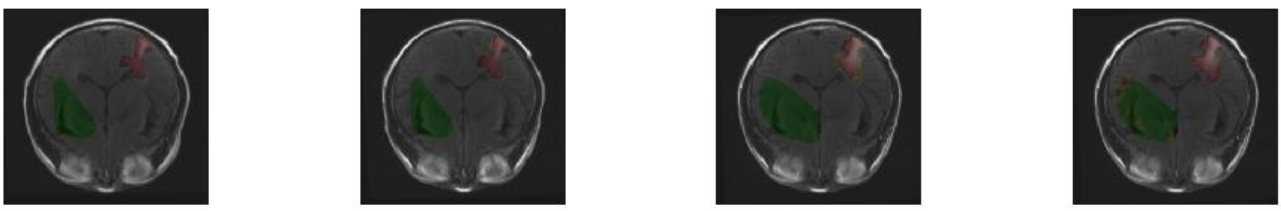

Figure 8. Prediction result on one sample slice for another patient. Images are arranged the same way as that in Figure 5.

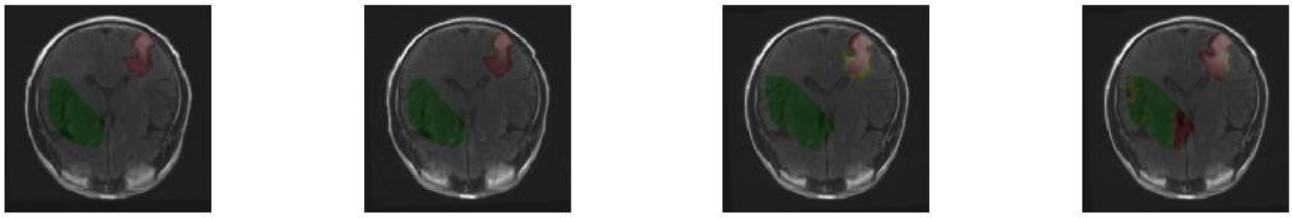

Figure 9. Prediction result on one sample slice for another patient. Images are arranged the same way as that in Figure 5.

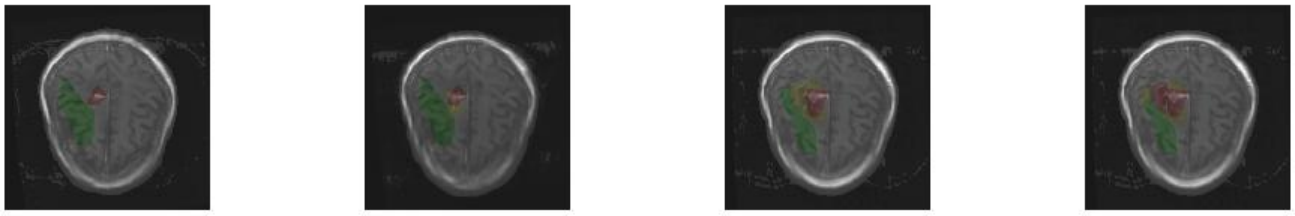

(a) (b) (c) (d)

(e) (f) (g) (h)

Figure 10. Prediction of brain tumor progression using histogram matched MRI images where tumor regions were defined on post contrast T1-wighted MRI slices. (a)-(c) and (e)-(g): Manually annotated contours, normal (green), tumor (red) and progression (yellow) at visit A, B and C, respectively. (d) and (h): Predicted results for tumor progressions at visit C using data at visit B (in Figures 10b and 10f) as inputs to the trained model.

(a) (b) (c) (d)

(e) (f) (g) (h)

Figure 11. A failed case. (a)-(c) and (e)-(g): Manually annotated contours, normal (green), tumor (red) and progression (yellow) at visit A, B and C, respectively, on a particular post contrast T1-weighted slices. (d) and (h), Predicted results for tumor progression at visit C using data at visit B as inputs to the trained model. Note that there are many highlighted regions at visit B (Figure 11b and 11f) and those in the annotated normal region are different from the corresponding region at visit A (Figure 11a and 11e). We suspect this is the reason the normal regions were classified as either tumor or progressed regions at visit C (Figure 11d and 11h).